JCB Article

DAP kinase and DRP-1 mediate membrane blebbing and the formation of autophagic vesicles during programmed cell death

Boaz Inbal,[1] Shani Bialik,[1] Ilana Sabanay,[2] Gidi Shani,[1] and Adi Kimchi[1]

[1]Department of Molecular Genetics and [2]Electron Microscopy Center, Weizmann Institute of Science, Rehovot 76100, Israel

Death-associated protein kinase (DAPk) and DAPk-related protein kinase (DRP)-1 proteins are Ca^{+2}/calmodulin–regulated Ser/Thr death kinases whose precise roles in programmed cell death are still mostly unknown. In this study, we dissected the subcellular events in which these kinases are involved during cell death. Expression of each of these DAPk subfamily members in their activated forms triggered two major cytoplasmic events: membrane blebbing, characteristic of several types of cell death, and extensive autophagy, which is typical of autophagic (type II) programmed cell death. These two different cellular outcomes were totally independent of caspase activity. It was also found that dominant negative mutants of DAPk or DRP-1 reduced membrane blebbing during the p55/tumor necrosis factor receptor 1–induced type I apoptosis but did not prevent nuclear fragmentation. In addition, expression of the dominant negative mutant of DRP-1 or of DAPk antisense mRNA reduced autophagy induced by antiestrogens, amino acid starvation, or administration of interferon-γ. Thus, both endogenous DAPk and DRP-1 possess rate-limiting functions in these two distinct cytoplasmic events. Finally, immunogold staining showed that DRP-1 is localized inside the autophagic vesicles, suggesting a direct involvement of this kinase in the process of autophagy.

Introduction

Programmed cell death has been classified based on morphological criteria into several categories (Kerr et al., 1972). The most extensively studied category, apoptosis, is characterized by cell rounding, membrane blebbing, cytoskeletal collapse, cytoplasmic condensation and fragmentation, nuclear pyknosis, chromatin condensation/fragmentation, and formation of membrane-bound apoptotic bodies that are rapidly phagocytosed and digested by macrophages or neighboring cells (Kerr et al., 1972; Wyllie et al., 1980; Clarke, 1990). A second prominent category is autophagic or type II cell death. Its main features are the appearance of abundant autophagic vacuoles in the cytoplasm, which is accompanied by mitochondrial dilation, and enlargement of the ER and the Golgi apparatus. Other hallmarks of type I apoptosis, such as nuclear pyknosis, membrane blebbing, and heterophagic elimination, either appear at later stages of the process or are less prevalent (for review see Clarke, 1990). The autophagic type of cell death has been visualized both in situ during development (for review see Clarke, 1990; Zakeri et al., 1995), in pathological situations, such as Alzheimer's (Cataldo et al., 1994) and Parkinson's diseases (Anglade et al., 1997), and in cell culture studies (Bursch et al., 1996; Jia et al., 1997; Christensen et al., 1998; Xue et al., 1999; Paglin et al., 2001). In some cases, apoptotic and autophagic cell death coincide in vivo in certain tissues (Clarke, 1990), and in rare cases both morphologies may coincide within the same cells (Jia et al., 1997; Christensen et al., 1998; Xue et al., 1999). Although much information has accumulated over the past decade about the genes and proteins which mediate some of the classical morphological changes during apoptosis, much less is known currently about the molecular mechanisms underlying other cytoplasmic changes, such as vacuolization or autophagy.

This study addresses the specific function of the death-associated protein kinase (DAPk)* family of genes, which have been shown previously to play a central role in various death signaling pathways. It focuses on two family members

Address correspondence to Adi Kimchi, Dept. of Molecular Genetics, Weizmann Institute of Science, Rehovot 76100, Israel. Tel.: 972-8-9342428. Fax: 972-8-9315938. E-mail: Adi.kimchi@weizmann.ac.il

Key words: DAP kinase; DRP-1; autophagy; membrane blebbing; programmed cell death

*Abbreviations used in this paper: CaM, calmodulin; DAPk, death-associated protein kinase; DRP, DAPk-related protein kinase; IFN, interferon; GFP, green fluorescent protein; MDC, monodansylcadaverin; PARP, poly (ADP-ribose) polymerase; ROCK, Rho-associated coiled-coil–containing protein kinase; TEM, transmission EM; TMRM, tetramethylrhodamine methyl ester; TNF, tumor necrosis factor; TNFR, TNF receptor.

which display the highest homology, DAPk (Deiss et al., 1995) and its closest homologue DAPk-related protein kinase (DRP)-1 (Kawai et al., 1999; Inbal et al., 2000; for review see Kogel et al., 2001). DAPk and DRP-1 are both Ca^{2+}-calmodulin (CaM)–regulated Ser/Thr kinases whose death-promoting activity relies on the catalytic domain activity (Cohen et al., 1997, 1999; Kawai et al., 1999; Inbal et al., 2000). DAPk additionally contains ankyrin repeats and the death domain motif and is localized to actin microfilaments (Deiss et al., 1995; Feinstein et al., 1995; Cohen et al., 1997). DRP-1, which is found in soluble cytosolic fractions, lacks these motifs and instead contains a 40 amino acid COOH-terminal tail that is required for homodimerization (Inbal et al., 2000; Shani et al., 2001). Thus, the homology between the two proteins is restricted to the kinase and CaM-binding domains. Interestingly, both kinases undergo a similar inhibitory autophosphorylation on a single conserved Ser within the CaM-binding domain, which inhibits the catalytic activation and restrains their death-promoting functions (Shani et al., 2001; Shohat et al., 2001). Several studies demonstrated the ability of DAPk to induce cell death in various cell lines and furthermore established that suppression of DAPk function slows down cell death triggered by various stimuli (e.g., interferon [IFN]-γ, tumor necrosis factor [TNF]-α, Fas, detachment from extracellular matrix, TGF-β, and C6-ceramide [Deiss et al., 1995; Cohen et al., 1997, 1999; Inbal et al., 1997; Jang et al., 2002; Pelled et al., 2002]). Other studies have linked the wide death-promoting effects of DAPk to its function as a tumor and a metastasis suppressor gene (Inbal et al., 1997; Kissil et al., 1997; Raveh et al., 2001). The latter paved the way to recent large scale cancer patient screens, which showed that DAPk expression is lost frequently in a wide range of tumor types (for review see Raveh and Kimchi, 2001). DRP-1 shares with DAPk some of the death-promoting functions, such as the participation in TNF-α cell death signaling (Inbal et al., 2000). The high degree of similarity in the catalytic and CaM regulatory domains of DAPk and DRP-1 suggests that they may share common substrates as evident by their joint ability to phosphorylate myosin light chain in in vitro kinase assays (Cohen et al., 1997; Kawai et al., 1999; Inbal et al., 2000). In addition, there is functional interaction between the two kinases, suggesting that they may be connected to similar subcellular outcomes (Inbal et al., 2000).

Here we found that DAPk and DRP-1 mediate the formation of autophagic vesicles that are characteristic of type II programmed cell death and also mediate a more prevalent event of cell death membrane blebbing. These two morphological events occur in a caspase-independent manner. DAPk family members are among the first identified death-promoting genes that regulate autophagy during type II cell death.

Results

DAPk family proteins induce membrane blebbing and the formation of autophagic vesicles

To follow the morphological characteristics of cell death resulting from expression of activated DAPk family proteins, various cell lines were transfected with constitutively active constructs of DAPk and DRP-1 (DAPk ΔCaM and DRP-1 Δ73, respectively). Cell death morphology was compared with that initiated by the well-characterized apoptotic (type I cell death) inducer, p55/TNF receptor (TNFR)1. Examination of the green fluorescent protein (GFP)-positive population of human kidney 293 cells at 24 h after transfection revealed that p55/TNFR1 induced cell rounding, membrane blebbing, detachment from the substrate, cytoplasmic condensation, and most prominently fragmentation of the whole cell into small apoptotic bodies (Fig. 1, A and B, 2). In contrast, 293 cells transfected with DAPk ΔCaM or DRP-1 Δ73 manifested only a restricted pattern of these cellular outcomes, including membrane blebbing, cell rounding, and partial detachment from the plate, whereas only rarely did cells condense and fragment into smaller apoptotic particles (Fig. 1, A and B, 3 and 4). Due to the lack of cytoplasmic condensation/fragmentation, the major phenotype which accumulated 24 h after transfection with each of the kinases was the blebbing phenotype, in contrast to the p55/TNFR1 transfectants in which a relatively smaller population of blebbed cells was evident. After prolonged incubation for 4–5 d, a slow process of bleb shedding occurred in the kinase-transfected cells, which resulted in the formation of round cells depleted of blebs rather than fragmented cells (unpublished data). Similar results were observed in kinase-transfected MCF-7 breast carcinoma cells, in SV80 fibroblasts, and in HeLa cells (unpublished data). To confirm that the blebbed cells indeed expressed the activated kinase on a single cell basis, we constructed a vector in which DAPk was fused to GFP at its NH_2 terminus. As shown in Fig. 1 C, the green DAPk-expressing cells displayed the blebbed phenotype, whereas the nontransfected cells within the same plate or cells transfected with GFP alone retained their normal spread morphology.

Differences in nuclear events were also observed after transfection with either p55/TNFR1 or DAPk family members. DAPI staining of p55/TNFR1-transfected 293 cells showed chromatin condensation and fragmentation of nuclei into small particles (Fig. 1 D, 6). In contrast, in DAPk ΔCaM and DRP-1 Δ73 transfections nuclei were only partially condensed without being further fragmented (Fig. 1 D, 4 and 5, respectively). Similar results were obtained in HeLa cells transfected with these kinases for 24 h (unpublished data). Moreover, no internucleosomal fragmentations of DNA were observed in DRP-1 Δ73– and DAPk ΔCaM–transfected cells (unpublished data). Altogether, these results emphasize that DAPk proteins induce membrane blebbing and a partial nuclear condensation without affecting the other type I apoptotic changes, such as cytoplasmic and complete nuclear condensation/fragmentation.

We next wished to test whether DAPk family proteins are connected to the mitochondrial signaling pathway. Neither DAPk nor DRP-1 reduced the mitochondrial membrane potential ($\Delta\Psi m$), in contrast to transfections with Bax used as a positive control (Fig. 2 A) (Xiang et al., 1996). Furthermore, in contrast to Bax-transfected cells in which cytochrome C was released from the mitochondria to the cytoplasm (Fig. 2 B, 3 and 5, for spread and blebbed cell morphologies, respectively) DRP-1– and DAPk-transfected blebbed cells continued to display punctate mitochondrial staining (Fig. 2 B, 7 and 9), similar to the staining observed

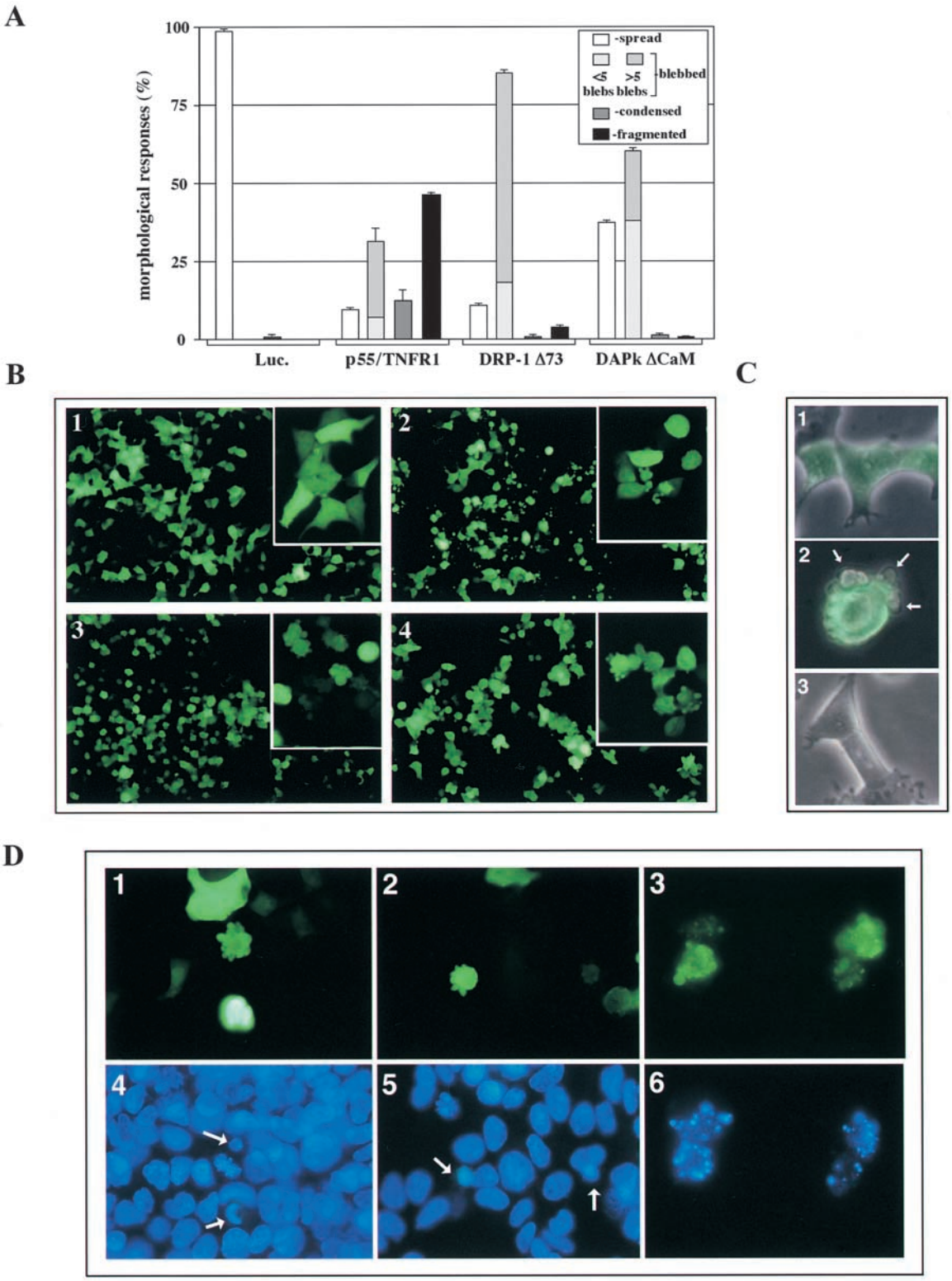

Figure 1. **Morphological changes induced by DAPk family proteins.** (A) Quantification of cell death in 293 cells 24 h after transfection with luciferase, p55/TNFR1, DRP-1 Δ73 or DAPk ΔCaM, and GFP. Graphs show the percentage of GFP-positive cells with altered cell morphology. (B) Photographs of GFP-positive cells cotransfected with luciferase (1), p55/TNFR1 (2), DRP-1 Δ73 (3), or DAPk ΔCaM (4). (C) Photographs showing the overlay of GFP and phase–contrast images of 293 cells 24 h after transfection with GFP and luciferase (1) or with GFP-DAPk (2 and 3); both a blebbing GFP-DAPk–expressing cell (2, arrows indicate blebs) and spread nontransfected cells are shown (3). (D) Hoechst staining (4–6) of GFP-positive 293 cells (1–3) 60 h after cotransfection with GFP and DAPk ΔCaM (1 and 4), DRP-1 Δ73 (2 and 5), or p55/TNFR1 (3 and 6). Arrows point to condensed nuclei resulting from DRP-1 Δ73 or DAPk ΔCaM transfections (4 and 5).

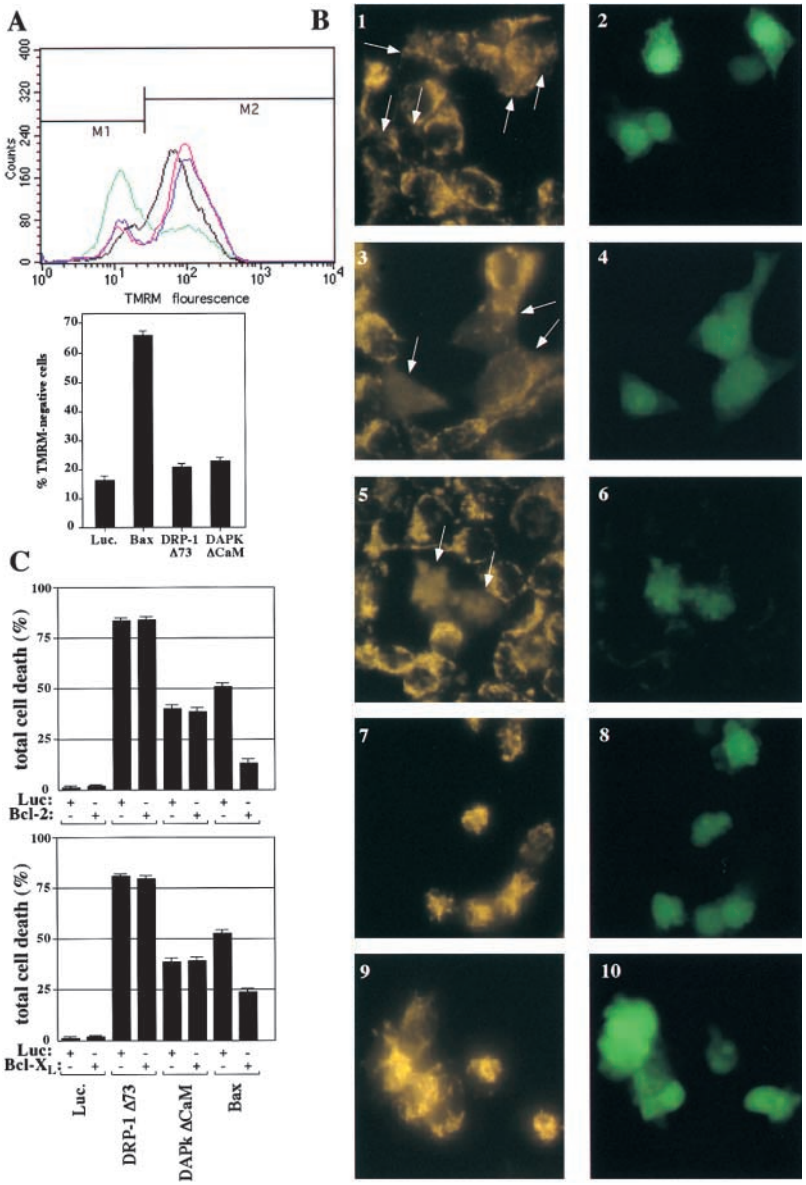

Figure 2. **DAPk family proteins do not induce cell death via the mitochondrial pathway.** (A) Scoring loss of mitochondrial membrane potential ($\Delta\Psi m$). 293 cells expressing luciferase (black), DRP-1 Δ73 (pink), DAPk ΔCaM (purple), and Bax (green) were assayed for loss of mitochondrial membrane potential 24 h after transfection using flow cytometric analysis of TMRM fluorescence. The fraction of TMRM-negative cells calculated from three experiments is shown in the graph below. The small increase in TMRM fluorescence in the kinase-transfected cells is not statistically significant. (B) Scoring the release of cytochrome C from mitochondria. 293 cells cotransfected with luciferase (1 and 2), Bax (3 and 6), DRP-1 Δ73 (7 and 8), or DAPk ΔCaM (9 and 10) and GFP constructs were incubated for 24 h and immunostained using anti–cytochrome C antibodies. Cells were visualized for cytochrome C (left) or GFP (right) fluorescence. Bax-transfected spread (3 and 4) or blebbed (5 and 6) cells are shown. In fields that also contain nontransfected cells, arrows point to GFP-positive cytochrome C–stained cells. (C) Assessing the effects of Bcl-2 and Bcl-X_L. 293 cells were cotransfected with luciferase, DRP-1 Δ73, DAPk ΔCaM, or Bax, and either Bcl-2 or Bcl-X_L together with GFP. GFP-positive cells were visualized by fluorescent microscopy and scored for the appearance of cell death morphology 24 h after transfection. Total cell death refers to the sum of all morphological changes observed.

in control luciferase-transfected cells (Fig. 2 B, 1). Also, upon cotransfection experiments Bcl-2 or Bcl-X_L failed to block the early effects induced by DAPk family proteins, such as membrane blebbing and partial detachment from the substrate, although they significantly inhibited the death effects of Bax (Fig. 2 C). These results rule out the direct involvement of mitochondrial events in this specific setting of DAPk family proteins' induced cell death.

To examine the morphological distinctions of DAPk family members' induced death in more detail, we analyzed 293 transfectants by transmission EM (TEM). p55/TNFR1-transfected cells showed membrane blebbing, mitochondrial darkening, chromatin clumping, and fragmentation (Fig. 3 A, 2a). At later stages, these cells were further condensed, engulfed by neighboring cells (Fig. 3 A, 2b), and completely phagocytosed (Fig. 3 A, 2c). In contrast, DRP-1 Δ73– and DAPk ΔCaM–transfected 293 cells were neither condensed and fragmented nor phagocytosed consistent with the light microscopy observations. In both cases, the kinase-transfected cells exhibited marked membrane blebbing. Additionally and quite surprisingly, a relatively high number of autophagic vesicles appeared (Fig. 3 A, 3a, 3b, and 4). These reflected different stages of autophagosomal development (Dunn, 1994), such as double membrane structures engulfing cytoplasmic matter and organelles (among them mitochondria were clearly identified), formation of mature autophagic vesicles and autolysosomes, and finally the degradation of interautophagic content, leading to the formation of a residual body (marked by double arrows, single black arrows, and dashed arrows, respectively). These autophagic vesicles could be mainly observed in perinuclear areas and less frequently inside the blebbed areas themselves (Fig. 3 A, 3a and 3b). In p55/TNFR1 transfections, autophagic vesicles were rarely observed (Fig. 3 A, 2a). DRP-1 Δ73–transfected 293 cells also displayed packed, yet uncondensed, unfragmented chromatin, disappearance of nuclear membranes, and in a few cases mixing between the organelles and the nuclear material (Fig. 3 A, 3a and 3b). Sim-

ilar results were observed in TEM studies of MCF-7 cells. Transfection of DRP-1 Δ73 or DAPk ΔCaM in these cells also resulted in the formation of autophagic vesicles in the cytoplasm (Fig. 3 B, 3a, 3b, and 4), packed chromatin that was only minimally condensed and rarely fragmented, and the disappearance of nuclear membranes resulting in mixing between the organelles and the nuclear material (Fig. 3 B, 3a, 3b, and 4). In contrast, the induction of cell death in MCF-7 cells by p55/TNFR1 expression resulted in a round cell morphology, chromatin condensation, and fragmentation (Fig. 3 B, 2a, 2b, and 2c) and condensation (darkening) of mitochondria similar to what has been described under conditions of high oxidative phosphorylation (Hackenbrock et al., 1971). At later stages, there was a marked packing and condensation of cytoplasmic constituents, including hundreds of empty vesicles, none of which were autophagic in nature (Fig. 3 B, 2c).

DRP-1 Δ 73–induced autophagy was quantified by scoring for the appearance of autophagic vesicles 48–72 h after transfection using the specific lysosomal/autophagic vacuole marker monodansylcadaverin (MDC) (Biederbick et al., 1995; Niemann et al., 2000). DRP-1 Δ73 expression statistically elevated MDC staining in both cell types (Fig. 4, A and B) in agreement with the TEM analysis of 293- and MCF-7–transfected cells described above. Thus, DRP-1 Δ73 induces autophagy-related elevation of MDC staining in 293 and MCF-7 cells in an analogous manner to the steroid withdrawal effect on MCF-7 cells (Bursch et al., 2000).

Effects of DAPk and DRP-1 on membrane blebbing and the formation of autophagic vesicles are caspase independent

To test whether caspases, in general, mediate the two major effects of DAPk and DRP-1 on membrane blebbing and autophagy, we performed transfections with DAPk ΔCaM and DRP-1 Δ73 in 293 and MCF-7 cells in the presence or absence of high doses of the pan-caspase inhibitors, BD-fmk and z-VAD-fmk (100 μM). As a positive control, we used p55/TNFR1 transfections, which are extremely sensitive to these pan-caspase inhibitors due to the rate-limiting effects of caspases both in the death-inducing signalling complex at the cell surface level and in further downstream events. Both caspase inhibitors blocked almost completely all phenotypic changes induced by p55/TNFR1 transfections in 293 and MCF-7 cells (Fig. 5 A and B, respectively), resulting in normal spread cell morphology (Fig. 5 D, 1). In contrast, these caspase inhibitors failed to alter the pattern of morphological changes induced by DAPk family members (Fig. 5, A and B). Similar results were obtained in cotransfection experiments using the cowpox caspase inhibitor crmA (Fig. 5 C). The lack of protection by caspase inhibitors was observed more closely in TEM studies of DAPk ΔCaM– and DRP-1 Δ73–transfected 293 cells exposed to 100 μM BD-fmk. As seen in Fig. 5 D, 2a and 2b, both membrane blebbing and the formation of autophagic vesicles at the different maturation stages were not affected at all by the addition of BD-fmk. In contrast, the p55/TNFR1 transfectants were fully protected and looked normal in the presence of BD-fmk with intact nuclei and cytoplasm and no signs of membrane blebbing (Fig. 5 D, 1). Western blot analysis of poly (ADP-ribose) polymerase (PARP), caspase-8, and caspase-3 cleavage in HeLa cells at 24 h after transfection demonstrated that these proteins were clearly processed in cells transfected with p55/TNFR1 but not in cells transfected with DRP-1 Δ73 or DAPk ΔCaM (Fig. 5 E). Together, these results demonstrate that caspases do not act downstream of DAPk family proteins in the pathway, which is responsible for membrane blebbing and autophagy.

DRP-1 and DAPk dominant negative mutants protect from p55/TNFR1-induced membrane blebbing in 293 cells

To further assess the involvement of endogenous DRP-1 and DAPk in the membrane blebbing process during programmed cell death, we transfected 293 cells with low amounts of p55/TNFR1 DNA (up to 20% of the levels used in the previous experiments shown in Figs. 1 and 5) to achieve a mild response and slow the cell fragmentation process. The effects of dominant negative mutants of DAPk or DRP-1 on the morphological responses to p55/TNFR1 were assessed upon cotransfection. For inhibition of DRP-1, the previously described K42A mutant was used (Inbal et al., 2000), whereas for DAPk we used a substructure of the DAPk death domain fused to GFP (Raveh et al., 2000). Cell death morphology of GFP-positive cells was followed 24 h later, and the percentage of blebbed cells was scored. Transfection of p55/TNFR1 induced ∼20–45% blebbed cells at 24 h. Each of the mutants effectively reduced the fraction of these cells, thus proving their relevance to the process (Fig. 6 A). To further extend the scoring of morphological changes, which are affected by DRP-1 K42A, the different morphological categories appearing during TNF-induced cell death (Fig. 6 B) were quantified. Transfection with DRP-1 K42A mutant by itself did not induce any morphological alterations, similar to the transfections with the control luciferase plasmid (Fig. 6 C, ∼100% spread cells). In the presence of low levels of p55/TNFR1, ∼45% of cells acquired the blebbed morphology, whereas another 15% had a condensed or fragmented cytoplasm. Although cotransfection with the K42A mutant strongly reduced the fraction of blebbed cells resulting from p55/TNFR1 expression, it did not interfere with the appearance of the condensed/fragmented cells. As a consequence, there was an increase in the proportions of both the normal spread cells and the fully condensed/fragmented cells (Fig. 6 C). Additionally, cotransfection with the K42A mutant induced the appearance of a novel morphology, which we named "nuclear-fragmented" cells (Fig. 6 B, 5). This category consisted of round cells lacking any signs of membrane blebbing or cytoplasmic condensation/fragmentation. Yet, they contained fragmented nuclei as determined by Hoechst 33342 staining (unpublished data). The appearance of this fraction of cells, though to a different extent in various experiments, suggests that mutant DRP-1 slows down cytoplasmic fragmentation relative to nuclear fragmentation, resulting in this intermediate phenotypic stage. Overall, these experiments suggest that DRP-1 and DAPk each display a rate-limiting function in the process of TNF-induced membrane blebbing.

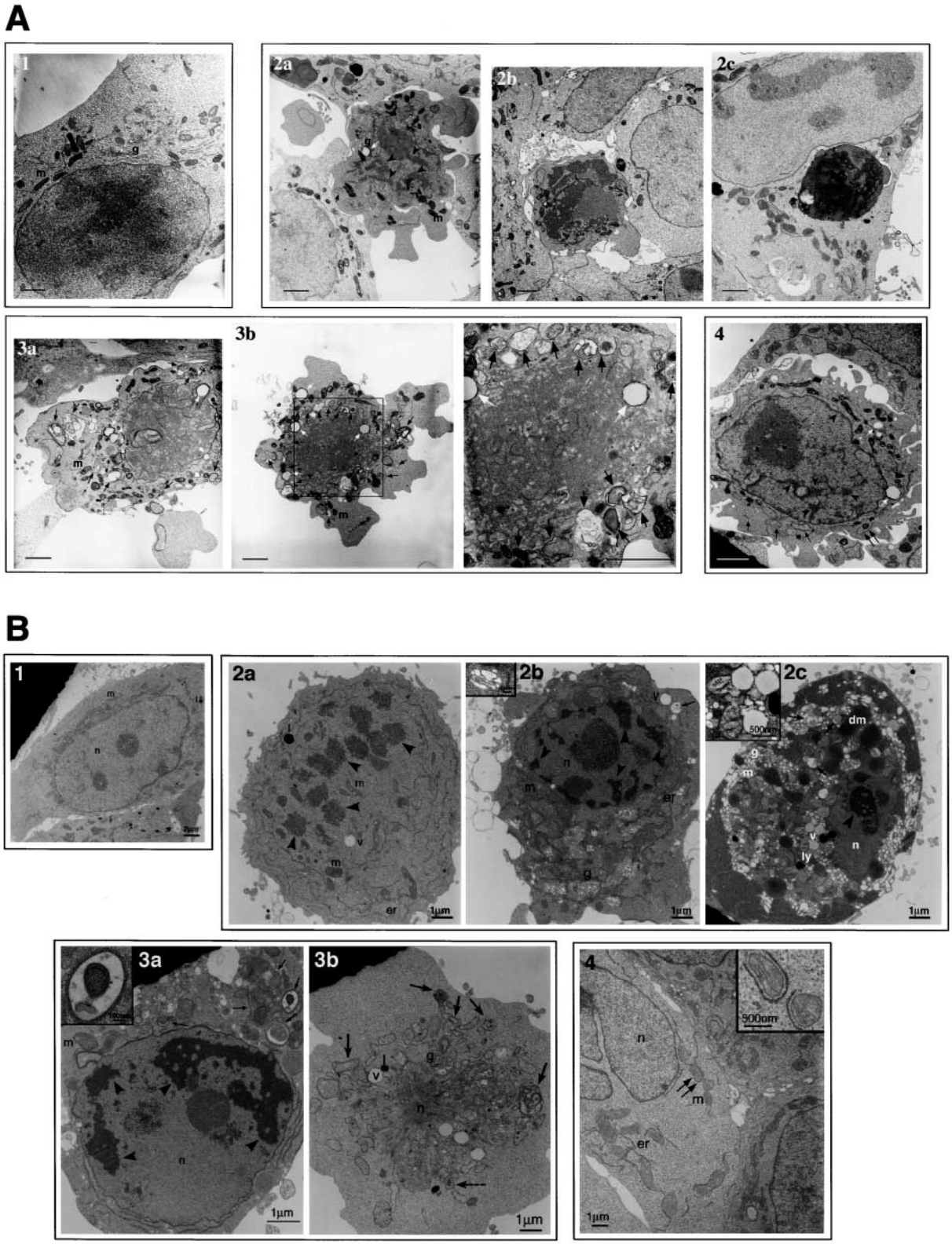

Figure 3. **High resolution morphology of DAPk family protein-induced cell death.** (A) Transmission electron micrographs of 293 cells transfected with luciferase (1) p55/TNFR1 (2a–2c), DRP-1 Δ73 (3a and 3b; part of fig. 3b is magnified on its right), and DAPk ΔCaM (4). The different stages of autophagic development are depicted as follows: immature autophagic vesicles (double arrow), mature autophagic vesicles and autolysosomes (black arrow), and residual bodies (dashed arrow). Empty vacuoles (white arrow) are also shown. Arrowheads show condensed and fragmented chromatin. m, mitochondria; g, Golgi apparatus. Bar, 1 μm. (B) Transmission electron micrographs of MCF-7 cells transfected with luciferase (1), p55/TNFR1 (2a–2c), DRP-1 Δ73 (3a and 3b), and DAPk ΔCaM (4). Immature autophagic vesicles (double arrow), autophagic vesicles (black arrow), and residual bodies (dashed arrow) are shown. Insets in B, 2b and 2c, correspond to empty vacuoles, whereas those in B, 3a and 4, correspond to autophagic vesicles. Arrowheads show condensed and fragmented chromatin. m, mitochondria; dm, darkened mitochondria; n, nucleus; g, Golgi apparatus; v, vacuoles; ly, lysosomes; er, endoplasmic reticulum.

Additionally, DRP-1 activity is not required for TNF-induced nuclear fragmentation.

DRP-1 K42A protects from the caspase-independent autophagy induced by steroid withdrawal and amino acid starvation of MCF-7 cells

The high abundance of autophagic vesicles in kinase-transfected cells and the lack of fragmentation and heterophagic elimination of dead cells suggest that some of the typical features of autophagic (type II) cell death might involve the DAPk family members, an hypothesis that was further studied in details in the following experiments. The dominant negative mutant form of DRP-1, DRP-1 K42A, was transiently expressed in MCF-7 cells, and these cells were then exposed to two stress stimuli known to induce autophagy (Bursch et al., 1996; Liang et al., 1999). DRP-1 K42A mutant partially blocked the appearance of MDC-positive cells and reduced the number of autophagic vesicles per cell upon steroid withdrawal by the antiestrogen tamoxifen (Fig. 7, A and C). Similar results were obtained upon amino acid starvation of MCF-7 cells (Fig. 7 B). These results demonstrate that DRP-1 is involved in stress-induced autophagy in the MCF-7 cell line.

Next, MCF-7 cells depleted of steroids were incubated in the presence of the broad caspase inhibitor BD-fmk (100 μM) to test the possible involvement of caspases. The administration of BD-fmk did not alter the percentage of MDC-positive cells (62 and 65% in BD-fmk–treated and nontreated cells, respectively) and the number of autophagic vesicles per cell (Fig. 8 A, 3 compared with 2 on the top). Similar results were also obtained in amino acid–starved MCF-7 cells (61 and 66% in BD-fmk–treated and nontreated cells, respectively) (Fig. 8 A, 5 compared with 4 on the bottom). Yet, autophagy could be inhibited by the general autophagy inhibitor 3-methyladenine (Seglen and Gordon, 1982), serving as a positive control for this assay and confirming the specificity of the MDC stainings (Fig. 8 A, 6 compared with 4 on the bottom). Furthermore, no traces of PARP cleavage were detected in these cells, unlike MCF-7 cells undergoing TNF-α–induced apoptosis (Fig. 8 B). At later stages of starvation, some cells are already shrunken and detached from the substrate. This autophagic cell death also could not be inhibited by 25 μM BD-fmk, z-DQMD-fmk, z-DEVD-fmk, or z-YVAD-fmk, implying a caspase-independent mode of cell death (Fig. 8 C). Moreover, within this selective population at late time points PARP cleavage was not observed (Fig. 8 B). Together, these experiments demonstrate that DRP-1 is involved in the type II cell death system of steroid withdrawal and amino acid starvation of MCF-7 cells and that these systems can proceed to terminal stages in a caspase-independent manner.

DAPk antisense RNA expression protects HeLa cells from IFN-γ–induced autophagy

DAPk protein was originally identified as a positive mediator of cell death induced by IFN-γ in HeLa cells using the TKO method developed in our laboratory (Deiss et al., 1995). Yet, it is not known whether IFN-γ induces features characteristic of autophagic cell death in these cells. HeLa cells were therefore treated with high doses of IFN-γ (1,000 U/ml) and were examined at day 2 (unpublished data) and 3 after their exposure to IFN-γ (Fig. 9, A and B). IFN-γ triggered a significant elevation in MDC-positive cells over the basal levels in nontreated cells and also increased the average number of autophagic vesicles per cell (Fig. 9 B, 2 compared with 1) in a caspase-independent manner (Fig. 9 B, 3 compared with 2). Unlike HeLa cells undergoing TNF-α–induced cell death, PARP was not cleaved in these cells (Fig. 9 C), thus suggesting that caspases were not activated in the course of IFN-γ–induced autophagic cell death. TEM analysis of IFN-γ–treated versus untreated cells further confirmed the marked induction of autophagic vesicles by IFN-γ (Fig. 9 D).

To verify more directly the role of DAPk in IFN-γ–induced autophagic cell death of HeLa cells, IFN-γ was administered (1,000 U/ml) to the DAPk antisense-transfected polyclonal population of HeLa cells and to the control DHFR-transfected cells that were generated previously in our laboratory in the course of the TKO screen (Deiss et al., 1995). The formation of autophagic vesicles in these two pairs of cell populations was compared by

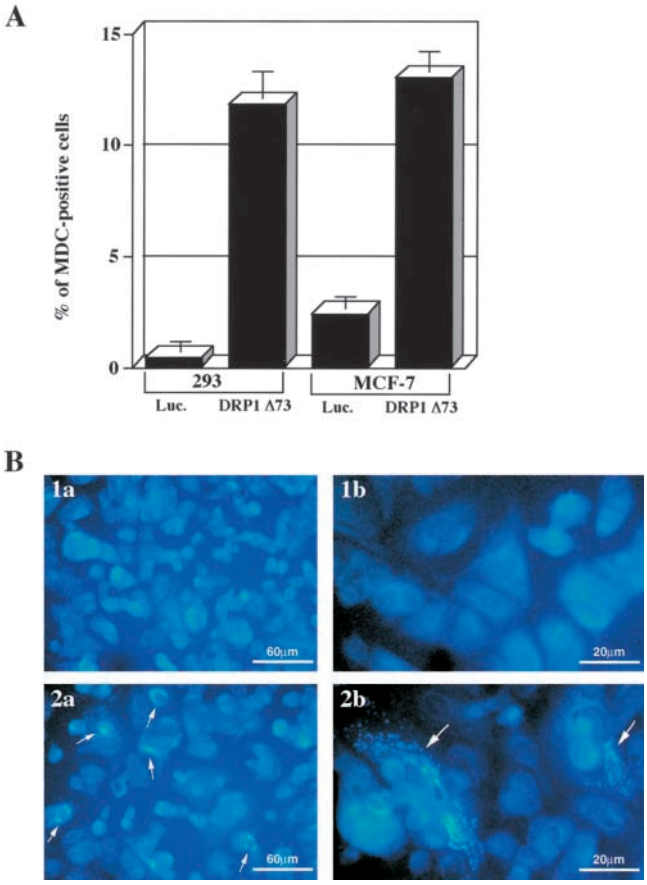

Figure 4. **DRP-1 induces autophagy in various cell lines.** (A) Quantification of autophagy in 293 and MCF-7 cells. Graphs show the percentage of MDC-positive cells resulting from luciferase or DRP-1 Δ73 transfections (mean ± SD calculated from triplicates of 100 cells each; note that total cell number comprises transfected and nontransfected cells). These experiments were repeated three times with reproducible results. (B) Photographs of MDC-stained MCF-7 cells from the same experiment shown in A. Arrows point to MDC-positive cells. Transfections: luciferase (1a and 1b) and DRP-1 Δ73 (2a and 2b) at low (a) and high (b) magnifications.

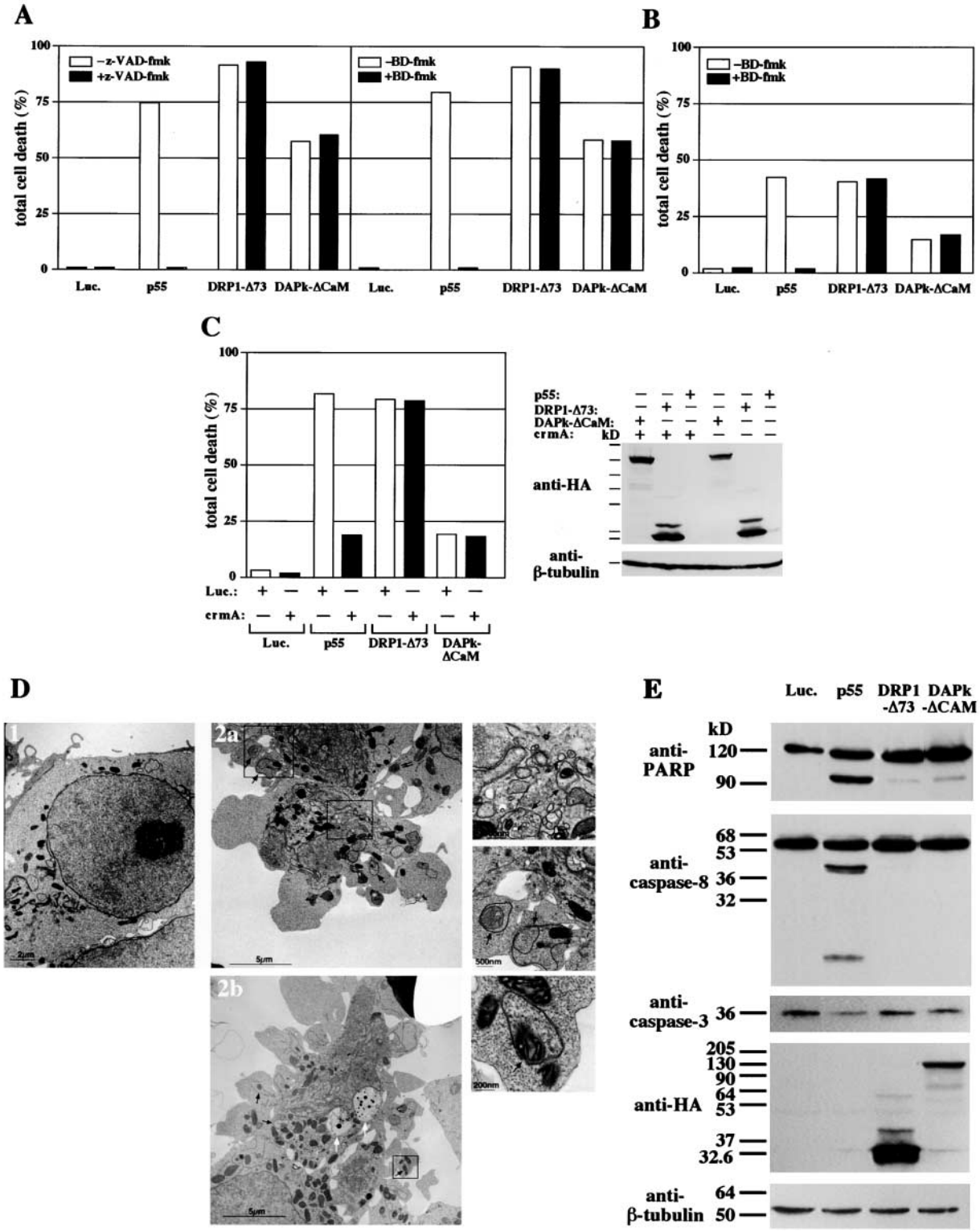

Figure 5. **DAPk family proteins induce caspase-independent cell death in various cell lines.** (A) Quantification of cell death-associated morphologies in 293 cells. Graphs show the percentage of cells harboring all spectrum of morphological changes occurring as a result of luciferase, p55/TNFR1, DRP-1 Δ73, or DAPk ΔCaM transfections in the presence or absence of the caspase inhibitors BD-fmk or z-VAD-fmk (100 μM; mean ± SD calculated from triplicates of 100 cells each). This experiment was repeated three times with reproducible results. (B) Quantification of cell death-associated morphologies in MCF-7 cells. Experimental conditions were performed as in A in the presence or absence of BD-fmk (100 μM). (C) Graphs show the percentage of cells harboring the complete spectrum of death-associated morphological changes occurring as a result of cotransfections of luciferase, p55/TNFR1, DRP-1 Δ73, or DAPk ΔCaM with the caspase inhibitor crmA or control luciferase vector (mean ± SD calculated from triplicates of 100 cells each). Immunoblot shows the expression levels of transfected HA-tagged DAPk and DRP-1 Δ73, confirming that cotransfection with crmA did not alter expression of the death-inducing proteins. (D) Transmission electron micrographs of 293 cells transfected with p55/TNFR1 (1) or DRP-1 Δ73 (2a and 2b; parts of these figures are magnified at the right) and treated with the caspase inhibitor BD-fmk (100 μM). Immature autophagic vesicles (double arrow), autophagic vesicles

MDC scoring. Although the increase in MDC-positive cells by IFN-γ in the DHFR-transfected populations was similar to that shown in Fig. 9 A, in antisense-transfected cells IFN-γ–induced autophagy was reduced significantly (Fig. 9 E). The caspase inhibitor BD-fmk did not inhibit autophagic vesicle formation in either case (Fig. 9 E), ruling out again the involvement of caspases in this type of cell death. These results imply that at least one of the protective modes of HeLa cells from IFN-γ–induced cell death by antisense DAPk RNA is via suppression of autophagic vesicle formation.

DRP-1 is localized to the inner part of autophagic and autolysosomic vesicles

To check the intracellular localization of DAPk and DRP-1 in 293 cells, immunogold labeling was used to detect HA epitope–tagged wild-type DAPk and DRP-1. In both TEM sections, a remarkable induction of autophagic vesicles was observed, similar to the previous results shown in Fig. 3. The immunogold staining of DAPk was mostly cytoplasmic without yielding a definitive pattern (unpublished data). In contrast, examination of DRP-1 transfectants, especially those which expressed moderate levels of the protein, clearly revealed that DRP-1 was specifically stained inside the lumen of autophagic/autolysosomal structures (Fig. 10, A–D). This staining was seen in autophagic vesicles harboring a double membrane and containing cytoplasmic matter (Fig. 10, A and B), in autophagic vesicles containing mitochondria and vacuoles (Fig. 10 C), and inside normal (Fig. 10 D) or large sized (unpublished data) autolysosomal structures. The gold particles did not overlap with the degraded organelles or lysosomes (Fig. 10, C and D). DRP-1 is therefore localized specifically inside autophagic/autolysosomal structures, implying a direct role in this process.

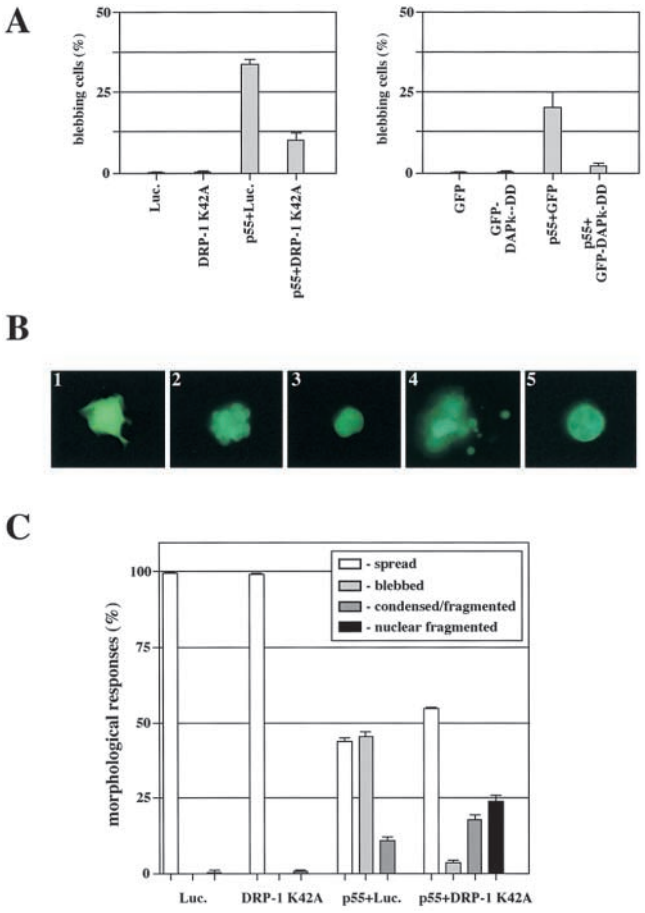

Figure 6. **DRP-1 and DAPk dominant negative mutants reduce membrane blebbing resulting from p55/TNFR1 transfections in 293 cells.** (A) 293 cells were cotransfected with p55/TNFR1 in combination with DAPk death domain fused to GFP or DRP-1 K42A and pEGFP-N1 vector. A control luciferase vector was also used. GFP-positive cells were visualized by fluorescent microscopy and scored for the appearance of membrane blebbing 24 h after transfection. (B) Photographs of the various categories of p55/TNFR1-transfected 293 cells: spread cells (1), blebbed cells (2), condensed cells (3), cells displaying a fragmented cytoplasm (4), and cells carrying fragmented nuclei within a noncondensed cytoplasm (5). (C) Quantification of each death morphology observed 24 h after transfection with GFP, p55/TNFR1, and either luciferase or DRP-1 K42A.

Discussion

In this study, we report that the activated forms of DAPk and DRP-1 are capable of inducing two distinct cytoplasmic events characteristic of programmed cell death: membrane blebbing and the formation of autophagic vesicles. Moreover, we show that by reducing the expression and/or activity of these DAPk family members both p55/TNFR-induced membrane blebbing and autophagy induced by multiple stimuli are significantly inhibited. This implies that the two kinases are necessary for bleb formation in apoptotic cells and for the formation of autophagic vesicles during autophagic cell death.

This work is part of our attempts to dissect at the subcellular level the different functional "arms" emanating from these death kinases. In a previous work, we found that in primary embryonic fibroblasts DAPk activates a strong and rapid cascade of caspase-dependent events, including DNA and cytoplasmic fragmentation (Raveh et al., 2001). This requires p53, which DAPk stabilizes and further activates in a p19ARF-dependent mechanism. As a consequence, the p53 pathway becomes the predominant functional arm in this system, and DAPk-induced cell death can be rescued by caspase inhibitors. Only in p53-deficient mouse embryonic fibroblasts in which the p53-mediated caspase-dependent mechanisms were not activated were alternate functional arms of DAPk apparent (Raveh et al., 2001). Here, the use of epithelial cell lines, which lack functional p53, enabled us to analyze the caspase-independent functions of DAPk family members, which include membrane blebbing and the formation of autophagic vesicles. It should be noted that in

(black arrow), and autolysosomes (white arrow) are shown. m, mitochondria; g, Golgi apparatus. (E) Western blots of cell lysates prepared from HeLa cells transfected with luciferase, p55/TNFR1, DRP-1 Δ73, or DAPk ΔCaM and GFP and incubated for 24 h. Blots were reacted with anti-PARP antibodies, anti–caspase-8 antibodies, anti–caspase-3 antibodies, anti-HA antibodies for DRP-1 Δ73 and DAPk ΔCaM detection, and anti–β-tubulin antibodies to quantitate protein loading.

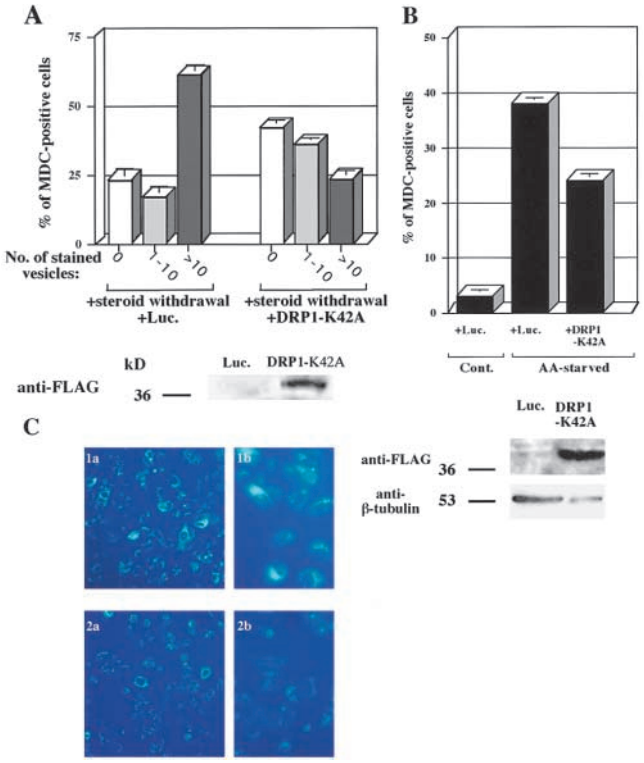

Figure 7. **DRP-1 K42A protects from autophagy induced by steroid withdrawal and amino acid starvation.** (A and B). Quantification of autophagy in MCF-7 cells. MCF-7 cells were transfected with luciferase or FLAG–DRP-1 K42A followed by steroid withdrawal (serum starvation plus 10^{-6} M tamoxifen treatment) (A) or by serum and amino acid starvation (B) (mean ± SD calculated from triplicates of 100 cells each). These experiments were repeated three times with reproducible results. Proteins extracted from the transfected cells were subjected to Western blot analysis with anti-FLAG and anti–β-tubulin antibodies. (C) Photographs of the MDC-stained steroid withdrawn MCF-7 cells taken from the same experiment shown in A. Transfections: luciferase (1a and 1b) and DRP-1 K42A (2a and 2b) at low (a) and high (b) magnifications.

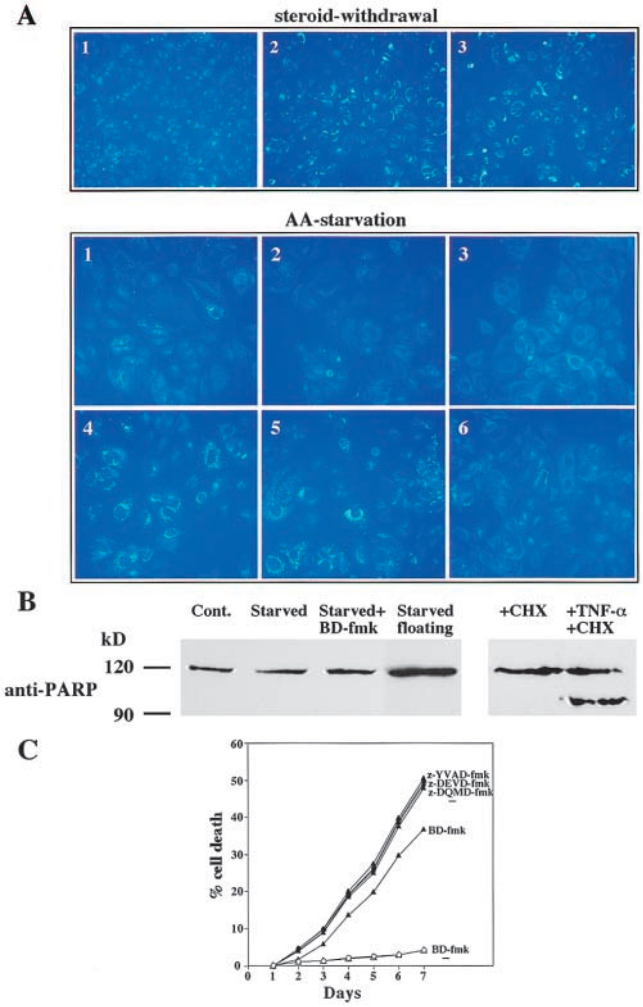

Figure 8. **Autophagy induced by steroid withdrawal or by amino acid starvation is insensitive to caspase inhibitors.** (A) Photographs of MDC-stained MCF-7 cells. (Top) Steroid withdrawal. Cells were either grown in complete medium (1), steroid depleted (2), or steroid depleted in the presence of the broad caspase inhibitor BD-fmk (100 μM) (3) for 3 d. (Bottom) amino acid starvation. Cells were either grown in complete medium (1–3) or under amino acid starvation condition (4–6) without (1 and 4) or with (2 and 5) the presence of the broad caspase inhibitor BD-fmk (100 μM) or the general inhibitor of autophagy 3-methyladenine (10 mM) (3 and 6) for 3 d. (B) PARP cleavage in MCF-7–starved cells. Proteins extracted from 4-d steroid-depleted (left) or 12-h TNF–α-treated (100 ng/ml) cells (right) were subjected to Western blot analysis with anti-PARP antibodies. The proteins were prepared from the same experiment shown in A. (C) Graph showing the cumulative phase microscopy scores of dead (shrunk and detached) MCF-7 cells in tamoxifen-treated (filled) or nontreated (unfilled) cultures in the presence (▲) or absence (●) of the indicated caspase inhibitors (25 μM).

these same cells, extremely high expression levels of DAPk are capable of inducing caspase-dependent events, which are suppressed by crmA and Bcl-2 (Cohen et al., 1999). Likewise, DAPk mediates a mitochondrial-based apoptotic pathway in response to TGFβ in a p53-deficient hepatoma cell line (Jang et al., 2002). Therefore, although DAPk in certain cell settings can be linked to caspase-dependent type I apoptotic cell death, it possesses an independent death function that can only be assessed in the absence of caspase activation as was seen in the experimental conditions presented here. These subcellular changes are sufficient to induce an irreversible commitment to cell death, since it was found that the number of colonies which appeared on plates after two weeks of culturing of kinase-transfected cells was reduced by several logs (unpublished data).

We show here for the first time that IFN-γ induces autophagic cell death in HeLa cells. Autophagy in HeLa cells and that induced by antiestrogen or amino acid starvation in MCF7 cells occurs independently of caspases, similar to newly isolated NGF-deprived superior cervical ganglia neurons and γ-irradiated MCF-7 cells (Xue et al., 1999; Paglin et al., 2001). This may dictate the slow progression of autophagic death in which the cells eventually die by the loss of essential organelles, such as mitochondria (Lemasters et al., 1998; Xue et al., 2001). Whereas rapid apoptosis ensures the immediate and quick elimination of hazardous cells, the slower nature of autophagic cell death may help to shape the tissue more accurately, enable enough time for a decision between cell survival and cell death in cases where minimal damage takes place, or simply allow cell death in cases where heterophagy is not available. Autophagic cell death probably represents a more ancient-based type of cell

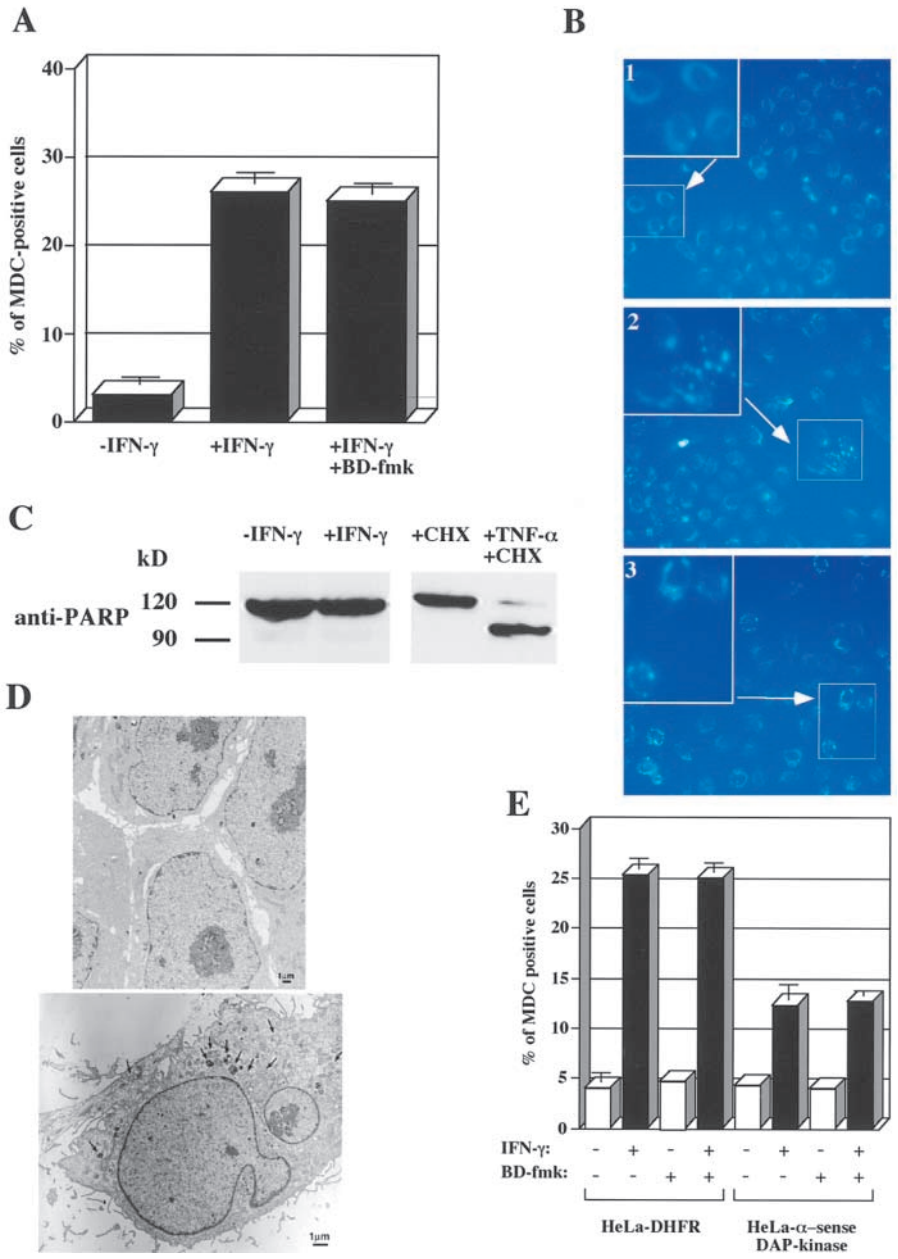

Figure 9. **DAPk antisense RNA protects from IFN-γ–induced autophagy of HeLa cells.** (A) Quantitation of autophagy in HeLa cells. Cells were either grown in complete medium (1), treated with IFN-γ (1,000 U/ml) (2), or treated with IFN-γ in the presence of the broad caspase inhibitor BD-fmk (100 μM) (3) for 3 d. (B) Photographs of the MDC-stained HeLa cells corresponding to the experiment in A. Treatments: complete medium (1), IFN-γ (1,000 U/ml) (2), and IFN-γ (1,000 U/ml) + BD-fmk (3). (C) PARP cleavage in HeLa IFN-γ–treated cells. Proteins extracted from IFN-γ–treated (left) or TNF-α–treated (100 ng/ml) cells (right) were subjected to Western blot analysis with anti-PARP antibodies. The proteins were prepared from the same experiment shown in A. (D) Transmission electron micrographs of nontreated (top) and IFN-γ–treated (bottom) HeLa cells. Arrows point to autophagic vesicles. (E) DAPk antisense-transfected and control DHFR-transfected polyclonal populations of HeLa cells were incubated with hygromycin B (200 μg/ml) in the presence or absence of IFN-γ (1,000 U/ml) and BD-fmk (50 μM). Detection of autophagic vesicles was performed 2 d later using the MDC dye. Graphs represent mean ± SD of MDC-positive cells calculated from triplicates of 100 cells each.

death (Klionsky and Emr, 2000), since many of the autophagy-associated genes are evolutionary conserved between yeast and mammalian organisms. Genes like DAPk or DRP-1, which do not exist in yeast, were probably added in evolution to provide a link between the basic evolutionary conserved autophagic machinery and programmed cell death. Another link between mammalian death-associated protein and the basic autophagy is provided by beclin 1, a tumor suppressor protein that interacts with Bcl-2 and is structurally similar to the yeast autophagic gene Apg6/Vps30p (Liang et al., 1998, 1999).

DRP-1 protein was localized to the lumen of autophagosomes and autolysosomes by immunogold staining. Since staining was not observed within the lysosomal compartment of the autolysosomes or within the engulfed organelles, we can conclude that DRP-1 is a resident protein of the autophagosome itself and was not nonspecifically delivered by lysosomes or the engulfed organelle. Of note, DRP-1 does not contain the peptide recognition signal KFERQ, which is used in the carrier-mediated proteolysis pathway (Dunn, 1994). Other mammalian proteins that localize to autophagosomes are involved in the structural stages of autophagic vesicle formation. These include the complex of mammalian Apg5p-Apg12p required for elongation of autophagic isolation membranes (Mizushima et al., 2001) and the mammalian homologue of yeast Apg8p, LC3, whose processed form is later targeted to autophagosome membranes (Kabeya et al., 2000). DRP-1's localization is consistent with it having a direct role in autophagosome formation, perhaps through phosphorylation of one or more of these autophagy-related proteins. In contrast, DAPk does not localize to the autophagosomes but rather is associated with actin microfilaments. DAPk may still influence the autophagic process through its association with the cytoskeletal structures that are involved in autophagosome formation (Dunn, 1994; Bursch et al.,

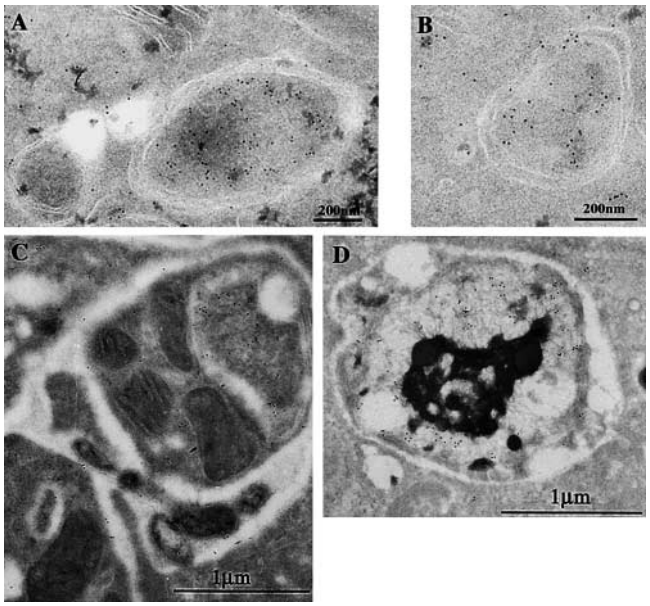

Figure 10. **DRP-1 is localized to the lumen of autophagic vesicles.** Immunogold staining of 293 cells expressing HA–DRP-1 reveals a specific staining of DRP-1 in the lumen of double membrane autophagosomes containing cytoplasmic material (A and B) in autophagosomes containing organelles and vacuoles (C) and inside the body of autolysosomes containing digested matter (D). The gold particles do not overlap with the phagocytosed organelles in C or the lysosomes in D.

2000). Thus, although both DAPk and DRP-1 are mediators of autophagy, the different intracellular localization of the two kinases suggests that they are not completely redundant in their mode of action.

Although DAPk and DRP-1 induce caspase-independent type II cell death, their functions are recruited by classical type I stimuli, such as TNF, to mediate membrane blebbing, a phenomenon common to both death processes. It has been proposed that during cell death myosin-mediated contraction of the cortical actin ring, occurring simultaneously with proteolytic degradation of cytoskeletal proteins that connect actin filaments to the cell membrane, gives rise to bleb extrusion in areas of structural weakness (Mills et al., 1998). Both kinases and a third family member, ZIP-kinase, are capable of phosphorylating the myosin regulatory light chain in vitro and in vivo on Ser19, a site responsible for activation of nonmuscle myosin (Cohen et al., 1997; Jin et al., 2001; Murata-Hori et al., 2001; Shani et al., 2001; unpublished data). Additional kinases that phosphorylate myosin light chain, such as the Rho-associated coiled-coil–containing protein kinase (ROCK), have been shown to mediate apoptotic membrane blebbing (Mills et al., 1998; Coleman et al., 2001; Sebbagh et al., 2001). Like DAPk and DRP-1, ROCK, once activated, was capable of inducing membrane blebbing in a caspase-independent manner. It will be important to precisely dissect the role of each of these kinases to determine whether there is cross talk between these pathways or whether each is a specific mediator of particular death signals. DAPk and DRP-1 are activated by the increase in intracellular Ca^{2+} (Cohen et al., 1997) and by means of dephosphorylation of autoinhibitory sites (Shani et al., 2001; Shohat et al., 2001), whereas ROCK activation during apoptosis requires caspase cleavage (Coleman et al., 2001; Sebbagh et al., 2001). Thus, DAPk protein members and ROCK could be differentially regulated in programmed cell death, depending on the nature of the trigger. For example, DAPk rather than ROCK may mediate the caspase-independent blebbing observed in Myc-induced death of Rat-1 cells (McCarthy et al., 1997).

Together, these results imply a major role of DAPk proteins in membrane blebbing and in the less studied process of autophagic (type II) cell death. Elucidating the exact molecular events taking place during this type of cell death, its cellular consequences, and relation to the apoptotic (type I) cell death are of primary importance for both scientific and clinical purposes.

Materials and methods

Transfections and apoptotic assays

Transient transfections were performed in 6-well dishes by the calcium-phosphate method or by SuperFect™ transfection reagent (QIAGEN). Except when GFP fusion proteins were used, all transfections included 0.5 μg of pEGFP-NI plasmid (CLONTECH Laboratories, Inc.) to mark the transfected population. For cell death assays by overexpression, 1.5 μg of pCDNA3 expressing p55/TNFR1, DRP-1 Δ73, or DAPk ΔCaM (Cohen et al., 1997; Inbal et al., 2000) was introduced per well. Alternatively, 2.0 μg of an in-frame fusion of DAPk to pEGFP-C2 (CLONTECH Laboratories, Inc.) was used. For cell death protection assays, a mixture of 0.5 μg of pCDNA3-p55/TNFR1, DRP-1 Δ73 or DAPk ΔCaM, and 1.5 μg of pCDNA3 expressing Bcl-2, Bcl-X_L, crmA or luciferase was used. For the membrane blebbing protection assays by DRP-1 or DAPk, cells were transfected with 0.1 or 0.3 μg p55/TNFR1, respectively, and 1.5 μg of either luciferase or pCDNA3-DRP-1 K42A (Inbal et al., 2000) or 2.5 μg of either pEGFP-CI or pEGFP-CI fused to a substructure of the DAPk death domain (Raveh et al., 2000). For the caspase-independent cell death assays, cells were treated 2–3 h after transfection with the caspase inhibitors z-VAD-fmk or BD-fmk (100 μM; Enzyme-Systems Products) or vehicle DMSO alone (1:500), left to grow for at least 24 h, and then visualized and scored for cell death morphology. For studies involving inhibition of autophagic cell death (see below), medium containing the caspase inhibitors BD-fmk, z-DQMD-fmk, z-DEVD-fmk or z-YVAD-fmk (25 μM; Enzyme-Systems Products) was replaced daily over a 3-d period. Nuclear staining was performed with DAPI (Cohen et al., 1997) or with Hoechst 33342 dye (0.2 μg/ml; Molecular Probes). Inverted fluorescent microscopy (IX70; Olympus) was performed with an excitation filter range of 470–490 nm or 360–370 nm and a barrier filter of 515 nm or 470–490 nm for GFP and Hoechst 33342/DAPI fluorescence, respectively.

Western blot analysis

Detection of proteins was performed by standard Western blot analysis using anti-HA antibodies (clone 16B12; Babco), anti-FLAG antibodies (M2; Sigma-Aldrich), anti-PARP antibodies (clone C-2–10; Biomol), anti–caspase-8 antibodies (clone 1C12; Cell Signaling), anti–caspase-3 antibodies (H-277; Santa Cruz Biotechnology), or anti–β-tubulin antibodies (clone TUB 2.1; Sigma-Aldrich).

Immunocytochemistry

Cells grown on coverslips were fixed in 4% paraformaldehyde for 15 min, permeabilized with 0.2% Triton in PBS for 10 min, and blocked with 10% normal goat serum in PBS for 30 min. Mouse monoclonal anti–cytochrome C antibodies were applied for 60 min (clone 6H2.B4; BD PharMingen) followed by Cy3-conjugated goat anti–mouse secondary antibodies (Jackson ImmunoResearch Laboratories) for 30 min. The coverslips were mounted in Mowiol and examined under transmitted light fluorescence microscope (Axioscope 2; ZEISS) with an excitation filter of 550–570 nm.

Loss of mitochondrial membrane potential

Cells transfected with the various death-inducing constructs were incubated 24 h after transfection with tetramethylrhodamine methyl ester (TMRM; 0.2 μM) (Molecular Probes) for 30 min at 37°C and then subjected to flow cytometry analysis using an argon-ion filter for TMRM detection (excitation wavelength at 514 nm, emission at 585 ± 21 nm). The mitochondrial uncoupler carbonyl cyanide p-trifluoromethoxyphenyl-hydrazone (10 μM; Sigma-Aldrich) was added 3 h before TMRM staining and was used as a positive control for mitochondrial depolarization.

Induction of type II cell death in MCF-7 breast carcinoma and HeLa cell lines

1×10^5 MCF-7 cells were seeded per 3-cm well and subjected to steroid depletion in the presence of 10^{-6} M tamoxifen (Sigma-Aldrich) for 3–5 d as described (Bursch et al., 1996). For amino acid starvation, cells were grown in Earle's balanced salt solution medium (GIBCO BRL) lacking amino acids and serum for 5–6 h with hourly replacement of the medium to discard secreted amino acids. HeLa cells (1×10^5/3-cm well) were treated with IFN-γ (1,000 μ/ml; Pepro Tech) for 2–3 d. Where indicated, MCF-7 cells were transfected with 1.5 μg dominant negative kinase DRP-1 K42A and 0.5 μg pEGFP-NI. 24 h later, cells were steroid depleted and left for another 24–48 h or AA-deprived for 5–6 h. Staining of autophagic vacuoles with 0.05 mM monodansylcadaverin (MDC; Sigma-Aldrich) was as described previously (Biederbick et al., 1995) and observed under inverted fluorescent microscope (IX50; Olympus) with an excitation filter range of 330–385 nm and a barrier filter of 420 nm.

TEM and immunogold staining

293 cells grown in 35-mm dishes were fixed for 60 min in Karnovsky's fixative (3% paraformaldehyde, 2% glutaraldehyde, 5 mM $CaCl_2$ in 0.1 M cacodylate buffer, pH 7.4, containing 0.1 M sucrose) and postfixed with 1% OsO_4, 0.5% potassium dichromate, and 0.5% potassium hexacyanoferrate in 0.1 M cacodylate buffer. The cells were stained en bloc with 2% aqueous uranyl acetate followed by ethanol dehydration. The dishes were embedded in Epon 812 (Tuosimis). Frontal sections were cut, stained with 2% uranyl acetate in 50% ethanol and lead citrate, and examined using a Philips CM-12 transmission electron microscope at an accelerating voltage of 100 KV. For immunogold detection of DRP-1 and DAPk, the transfected 293 cells grown in 90-mm Falcon dishes were fixed in situ for 1 h at 24°C in a freshly prepared solution of Karnovsky's fixative. Scraped cell pellets were then incubated in 10% gelatin at 37°C for 30 min and centrifuged at 37°C. Excess gelatin was removed, and pellets were postfixed in Karnovsky's fixative overnight at 4°C. The pellets were cut into small pieces and cryoprotected by overnight infiltration with 2.3 M sucrose in 0.1 M cacodylate buffer. Samples were quick frozen in liquid nitrogen, and ultrathin frozen sections (75 nm) were cut at 110°C on Reichert Ultracat-S ultramicrotome. The sections were transferred to formvar-coated 200 mesh nickel grids and blocked with conditional medium as described (Tokuyasu, 1980). Sections were incubated with rabbit anti-HA antibodies (1:100–200; Santa Cruz Biotechnology) for 2 h. After extensive washing in PBS-0.1% glycine, the primary antibodies were detected with goat anti–rabbit 10 nm colloidal gold conjugate (1:20; Zymed Laboratories). The grids were then washed in PBS-glycine, stained with neutral uranyl acetate oxalate for 5 min, and then stained with 2% uranyl acetate in H_2O for 10 min. They were then embedded in 2% methyl cellulose/uranyl acetate as described (Tokuyasu, 1980).

We thank O. Yeger for technical assistance in TEM, D. Wallach for providing anti–caspase-8 antibodies and the pCDNA3-p55/TNFR1 construct, S.J Korsmeyer for the pCDNA3-Bcl-2 and pCDNA3-Bcl-X_L constructs, and A. Gross for the Bax plasmid.

This work was supported by a grant from Deutsch-Israelische Projektkooperation. A. Kimchi is the incumbent of Helena Rubinstein Chair of Cancer Research.

Submitted: 26 September 2001
Revised: 19 March 2002
Accepted: 25 March 2002

References

Anglade, P., S. Vyas, F. Javoy-Agid, M.T. Herrero, P.P. Michel, J. Marquez, A. Mouatt-Prigent, M. Ruberg, E.C. Hirsch, and Y. Agid. 1997. Apoptosis and autophagy in nigral neurons of patients with Parkinson's disease. *Histol. Histopathol.* 12:25–31.

Biederbick, A., H.F. Kern, and H.P. Elsasser. 1995. Monodansylcadaverine (MDC) is a specific in vivo marker for autophagic vacuoles. *Eur. J. Cell Biol.* 66:3–14.

Bursch, W., A. Ellinger, H. Kienzl, L. Torok, S. Pandey, M. Sikorska, R. Walker, and R.S. Hermann. 1996. Active cell death induced by the anti-estrogens tamoxifen and ICI 164 384 in human mammary carcinoma cells (MCF-7) in culture: the role of autophagy. *Carcinogenesis.* 17:1595–1607.

Bursch, W., K. Hochegger, L. Torok, B. Marian, A. Ellinger, and R.S. Hermann. 2000. Autophagic and apoptotic types of programmed cell death exhibit different fates of cytoskeletal filaments. *J. Cell Sci.* 113:1189–1198.

Cataldo, A.M., D.J. Hamilton, and R.A. Nixon. 1994. Lysosomal abnormalities in degenerating neurons link neuronal compromise to senile plaque development in Alzheimer disease. *Brain Res.* 640:68–80.

Christensen, S.T., J. Chemnitz, E.M. Straarup, K. Kristiansen, D.N. Wheatley, and L. Rasmussen. 1998. Staurosporine-induced cell death in *Tetrahymena thermophila* has mixed characteristics of both apoptotic and autophagic degeneration. *Cell Biol. Int.* 22:591–598.

Clarke, P.G. 1990. Developmental cell death: morphological diversity and multiple mechanisms. *Anat. Embryol (Berl.)* 181:195–213.

Cohen, O., E. Feinstein, and A. Kimchi. 1997. DAPk is a Ca2+/calmodulin-dependent, cytoskeletal-associated protein kinase, with cell death-inducing functions that depend on its catalytic activity. *EMBO J.* 16:998–1008.

Cohen, O., B. Inbal, J.L. Kissil, T. Raveh, H. Berissi, T. Spivak-Kroizaman, E. Feinstein, and A. Kimchi. 1999. DAPk participates in TNF-α– and Fas-induced apoptosis and its function requires the death domain. *J. Cell Biol.* 146:141–148.

Coleman, M.L., E.A. Sahai, M. Yeo, M. Bosch, A. Dewar, and M.F. Olson. 2001. Membrane blebbing during apoptosis results from caspase-mediated activation of ROCK I. *Nat. Cell Biol.* 3:339–345.

Deiss, L.P., E. Feinstein, H. Berissi, O. Cohen, and A. Kimchi. 1995. Identification of a novel serine/threonine kinase and a novel 15-kD protein as potential mediators of the gamma interferon-induced cell death. *Genes Dev.* 9:15–30.

Dunn, W.A., Jr. 1994. Autophagy and related mechanisms of lysosome-mediated protein degradation. *Trends Cell Biol.* 4:139–143.

Feinstein, E., A. Kimchi, D. Wallach, M. Boldin, and E. Varfolomeev. 1995. The death domain: a module shared by proteins with diverse cellular functions. *Trends Biochem. Sci.* 20:342–344.

Hackenbrock, C.R., T.G. Rehn, E.C. Weinbach, and J.J. Lemasters. 1971. Oxidative phosphorylation and ultrastructural transformation in mitochondria in the intact ascites tumor cell. *J. Cell Biol.* 51:123–137.

Inbal, B., O. Cohen, S. Polak-Charcon, J. Kopolovic, E. Vadai, L. Eisenbach, and A. Kimchi. 1997. DAP kinase links the control of apoptosis to metastasis. *Nature.* 390:180–184.

Inbal, B., G. Shani, O. Cohen, J.L. Kissil, and A. Kimchi. 2000. Death-associated protein kinase-related protein 1, a novel serine/threonine kinase involved in apoptosis. *Mol. Cell. Biol.* 20:1044–1054.

Jang, C.W., C.H. Chen, C.C. Chen, J.Y. Chen, Y.H. Su, and R.H. Chen. 2002. TGF-beta induces apoptosis through Smad-mediated expression of DAPk. *Nat. Cell Biol.* 4:51–58.

Jia, L., R.R. Dourmashkin, P.D. Allen, A.B. Gray, A.C. Newland, and S.M. Kelsey. 1997. Inhibition of autophagy abrogates tumour necrosis factor alpha induced apoptosis in human T-lymphoblastic leukaemic cells. *Br. J. Haematol.* 98:673–685.

Jin, Y., E.K. Blue, S. Dixon, L. Hou, R.B. Wysolmerski, and P.J. Gallagher. 2001. Identification of a new form of death associated protein kinase that promotes cell survival. *J. Biol Chem.* 276:39667–39678.

Kabeya, Y., N. Mizushima, T. Ueno, A. Yamamoto, T. Kirisako, T. Noda, E. Kominami, Y. Ohsumi, and T. Yoshimori. 2000. LC3, a mammalian homologue of yeast Apg8p, is localized in autophagosome membranes after processing. *EMBO J.* 19:5720–5728.

Kawai, T., F. Nomura, K. Hoshino, N.G. Copeland, D.J. Gilbert, N.A. Jenkins, and S. Akira. 1999. Death-associated protein kinase 2 is a new calcium/calmodulin-dependent protein kinase that signals apoptosis through its catalytic activity. *Oncogene.* 18:3471–3480.

Kerr, J.F., A.H. Wyllie, and A.R. Currie. 1972. Apoptosis: a basic biological phenomenon with wide-ranging implications in tissue kinetics. *Br. J. Cancer.* 26:239–257.

Kissil, J.L., E. Feinstein, O. Cohen, P.A. Jones, Y.C. Tsai, M.A. Knowles, M.E. Eydmann, and A. Kimchi. 1997. DAPk loss of expression in various carcinoma and B-cell lymphoma cell lines: possible implications for role as tumor suppressor gene. *Oncogene.* 15:403–407.

Klionsky, D.J., and S.D. Emr. 2000. Autophagy as a regulated pathway of cellular degradation. *Science.* 290:1717–1721.

Kogel, D., J.H. Prehn, and K.H. Scheidtmann. 2001. The DAP kinase family of pro-apoptotic proteins: novel players in the apoptotic game. *Bioessays.* 23:352–358.

Lemasters, J.J., A.L. Nieminen, T. Qian, L.C. Trost, S.P. Elmore, Y. Nishimura, R.A. Crowe, W.E. Cascio, C.A. Bradham, D.A. Brenner, and B. Herman. 1998. The mitochondrial permeability transition in cell death: a common mechanism in necrosis, apoptosis and autophagy. *Biochim. Biophys. Acta.* 1366:177–196.

Liang, X.H., L. Kleeman, H.H. Jiang, G. Gordon, J.E. Goldman, G. Berry, B. Herman, and B. Levine. 1998. Protection against fatal Sindbis virus encephalitis by Beclin, a novel Bcl-2-interacting protein. *J. Virol.* 72:8586–8596.

Liang, X.H., S. Jackson, M. Seaman, K. Brown, B. Kempkes, H. Hibshoosh, and B. Levine. 1999. Induction of autophagy and inhibition of tumorigenesis by beclin 1. *Nature.* 402:672–676.

McCarthy, N.J., M.K. Whyte, C.S. Gilbert, and G.I. Evan. 1997. Inhibition of Ced-3/ICE-related proteases does not prevent cell death induced by oncogenes, DNA damage, or the Bcl-2 homologue Bak. *J. Cell Biol.* 136:215–227.

Mills, J.C., N.L. Stone, J. Erhardt, and R.N. Pittman. 1998. Apoptotic membrane blebbing is regulated by myosin light chain phosphorylation. *J. Cell Biol.* 140:627–636.

Mizushima, N., A. Yamamoto, M. Hatano, Y. Kobayashi, Y. Kabeya, K. Suzuki, T. Tokuhisa, Y. Ohsumi, and T. Yoshimori. 2001. Dissection of autophagosome formation using Apg5-deficient mouse embryonic stem cells. *J. Cell Biol.* 152:657–668.

Murata-Hori, M., Y. Fukuta, K. Ueda, T. Iwasaki, and H. Hosoya. 2001. ZIP kinase induces diphosphorylation of myosin II regulatory light chain and reorganization of actin filaments in nonmuscle cells. *Oncogene.* 20:8175–8183.

Niemann, A., A. Takatsuki, and H.P. Elsasser. 2000. The lysosomotropic agent monodansylcadaverine also acts as a solvent polarity probe. *J. Histochem. Cytochem.* 48:251–258.

Paglin, S., T. Hollister, T. Delohery, N. Hackett, M. McMahill, E. Sphicas, D. Domingo, and J. Yahalom. 2001. A novel response of cancer cells to radiation involves autophagy and formation of acidic vesicles. *Cancer Res.* 61:439–444.

Pelled, D., T. Raveh, C. Riebeling, M. Fridkin, H. Berissi, A.H. Futerman, and A. Kimchi. 2002. Death-associated protein (DAP) kinase plays a central role in ceramide-induced apoptosis in cultured hippocampal neurons. *J. Biol. Chem.* 277:1957–1961.

Raveh, T., and A. Kimchi. 2001. DAP kinase-a proapoptotic gene that functions as a tumor suppressor. *Exp. Cell Res.* 264:185–192.

Raveh, T., H. Berissi, M. Eisenstein, T. Spivak, and A. Kimchi. 2000. A functional genetic screen identifies regions at the C-terminal tail and death-domain of death-associated protein kinase that are critical for its proapoptotic activity. *Proc. Natl. Acad. Sci. USA.* 97:1572–1577.

Raveh, T., G. Droguett, M.S. Horwitz, R.A. DePinho, and A. Kimchi. 2001. DAP kinase activates a p19ARF/p53-mediated apoptotic checkpoint to suppress oncogenic transformation. *Nat. Cell Biol.* 3:1–7.

Sebbagh, M., C. Renvoize, J. Hamelin, N. Riche, J. Bertoglio, and J. Breard. 2001. Caspase-3-mediated cleavage of ROCK I induces MLC phosphorylation and apoptotic membrane blebbing. *Nat. Cell Biol.* 3:346–352.

Seglen, P.O., and P.B. Gordon. 1982. 3-Methyladenine: specific inhibitor of autophagic/lysosomal protein degradation in isolated rat hepatocytes. *Proc. Natl. Acad. Sci. USA.* 79:1889–1892.

Shani, G., S. Henis-Korenblit, G. Jona, O. Gileadi, M. Eisenstein, T. Ziv, A. Admon, and A. Kimchi. 2001. Autophosphorylation restrains the apoptotic activity of DRP-1 kinase by controlling dimerization and calmodulin binding. *EMBO J.* 20:1099–1113.

Shohat, G., T. Spivak, S. Bialik, O. Cohen, G. Shani, M. Eisenstein, and A. Kimchi. 2001. A novel mechanism of negative autophosphorylation restrains the pro-apoptotic function of DAPk J. *Biol. Chem*. 276: 47450–47467.

Tokuyasu, K.T. 1980. Immunochemistry on ultrathin frozen sections. *Histochem. J.* 12:381–403.

Wyllie, A.H., J.F. Kerr, and A.R. Currie. 1980. Cell death: the significance of apoptosis. *Int. Rev. Cytol.* 68:251–306.

Xiang, J., D.T. Chao, and S.J. Korsmeyer. 1996. BAX-induced cell death may not require interleukin 1 beta-converting enzyme-like proteases. *Proc. Natl. Acad. Sci. USA.* 93:14559–14563.

Xue, L., G.C. Fletcher, and A.M. Tolkovsky. 1999. Autophagy is activated by apoptotic signalling in sympathetic neurons: an alternative mechanism of death execution. *Mol. Cell. Neurosci.* 14:180–198.

Xue, L., G.C. Fletcher, and A.M. Tolkovsky. 2001. Mitochondria are selectively eliminated from eukaryotic cells after blockade of caspases during apoptosis. *Curr. Biol.* 11:361–365.

Zakeri, Z., W. Bursch, M. Tenniswood, and R. Lockshin. 1995. Cell death: programmed, apoptosis, necrosis, or other? *Cell Death Diff.* 2:87–96.